Wing Rock Suppression Using Recessed Angle Spanwise Blowing

A. G. Sreenatha* and T. K. Ong†
Australian Defence Force Academy, Canberra, Australian Capital Territory 2600, Australia

Introduction

ONE of the limitations to combat effectiveness of fighter aircraft is wing rock—a high angle-of-attack dynamic motion manifested primarily in a limit-cycle roll oscillations phenomenon.[1] It is an aerodynamic phenomenon that causes loss of stability and control in the lateral/directional mode. The leading-edge vortices emanating from the high-performance fighter aircraft are one of the main causes of wing rock at high angles of attack. An effective means of suppressing wing rock is through the direct control and manipulation of leading-edge vortices at these flight regimes. The technique of "blowing"[2–4] has been of greatest interest because it is found to be highly effective in controlling the vortex orientation. This Note involves the experimental implementation of one such blowing technique—recessed angle spanwise blowing (RASB),[3] using a simple rule base controller to a slender delta wing model in a low-turbulence wind tunnel. Through interpretation of the observations and results obtained from the experiments, an analysis is conducted to assess the effectiveness of RASB in suppressing wing rock. The results are substantiated by the flow visualization experiments and force balance experiments. The excellent correlations of the results and observations demonstrate the effectiveness of the RASB technique in its stipulated role of wing rock suppression.

Experimental Setup

The delta wing has a sharp leading edge with an 80-deg sweep angle and an aspect ratio of 0.705. The wing is constructed from aluminium and weighs 113 g. Two symmetrical longitudinally separated chambers of thickness 1.5 mm lie in between the wing surfaces to provide the cavities for air passage through the left or right wing. Twelve blowing ports of 1.0 mm in diameter each are drilled in each side of the wing at the same bevelled angle of 45 deg to the wing surface (Fig. 1). The slender delta-wing model is mounted on low-friction bearings to allow it to rotate freely about its longitudinal axis. The block diagram of the experimental setup is given in Fig. 2. The rule base controller is incorporated in the PC.

The electronic proportional directional control valve has two output channels that are connected to each side of the wing through rubber tubes. The valve-slide stroke of this control valve can be controlled to a specified set point by an analog electrical input signal. Thus, the control valve can control the flow rate of the pressurized air supply as regards to both its magnitude and direction. An electrical input signal from the simple rule-based controller in the PC commands the switching of the valve-slide stroke between its two output channels to supply the air into either side of the wing at the required pressure.

Rule-Based Controller

The control valve determines the direction and magnitude of the blowing during different phases of the wing rock motion. For this, a simple rule-based controller is developed by experimentation. The rule base is constructed based on the phase of the roll angle. Each cycle of the wing rock motion is divided into four main quarters as shown in Fig. 3. By convention, roll angle is positive when the wing is rolling to the right. During each quarter of the cycle, there are three possible options of control input, namely, blowing in the left wing, blowing in the right wing, or no blowing in either side of the wing.

The schematic representation of a typical rule base is also given in Fig. 3. Positive control input refers to blowing in the right wing. Representing the control input in each quarter of the wing rock as seen in Fig. 3, the rule base is summarized as RNLN, where R stands for blowing in the right wing, N for no blowing, and L for blowing in the left wing.

Experimental Simulations

The flow visualization experiment is conducted to map the leading-edge vortices above the wing model during static and dynamic conditions. A laser-sheet generator is used to generate a laser sheet perpendicular to the model longitudinal axis at various streamwise positions. A smoke generator located upstream of the model in the wind tunnel is used to illuminate the flow by the laser sheet scattering off the smoke particles. The laser sheet is placed on the second set of holes (at a distance of 56 mm from the leading edge). High-resolution and high-speed digital cameras are used to record the flow visualization. All of the results are presented at 22.5 deg angle of attack.

Figure 4 illustrates the flowfield over the wing model when the model is at three different roll angles. The vortex at the higher side of the wing is always larger than the vortex at the lower side of the wing. This is expected because the lift at the higher wing must be greater than the lower wing. In addition, the position of the larger vortex appears to be further away from the wing. It is also evident that the vortex position of the higher wing is further outboard of the wing. These observations are in accordance with the theory postulated by Arena and Nelson.[5–7] Figure 4c indicates the symmetrical vortices in the equilibrium condition.

Figure 5 demonstrates the effects of blowing on the vortical flowfield. Image a) indicates a growth of the vortex size on the right wing

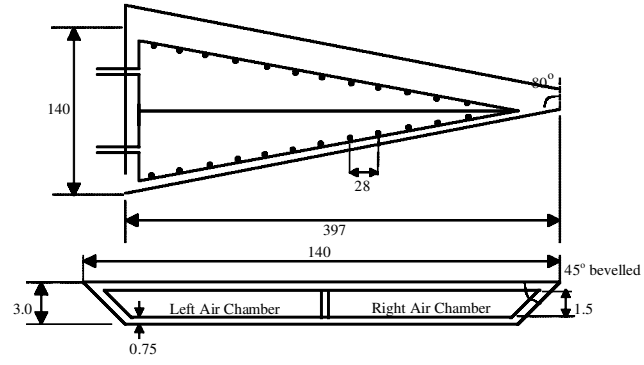

Fig. 1 Schematic plan view and back view of the slender delta-wing model. (All dimensions are in millimeters; not drawn to scale.)

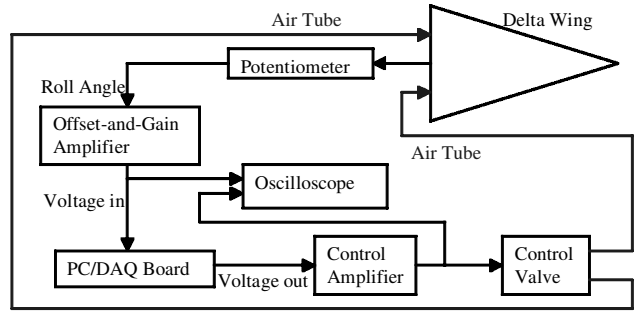

Fig. 2 Block diagram of the control system.

Received 30 July 2001; revision received 28 May 2002; accepted for publication 29 May 2002.

*Senior Lecturer, School of Aerospace and Mechanical Engineering, University College, Northcott Drive.

†Undergraduate Student, School of Aerospace and Mechanical Engineering, University College, Northcott Drive.

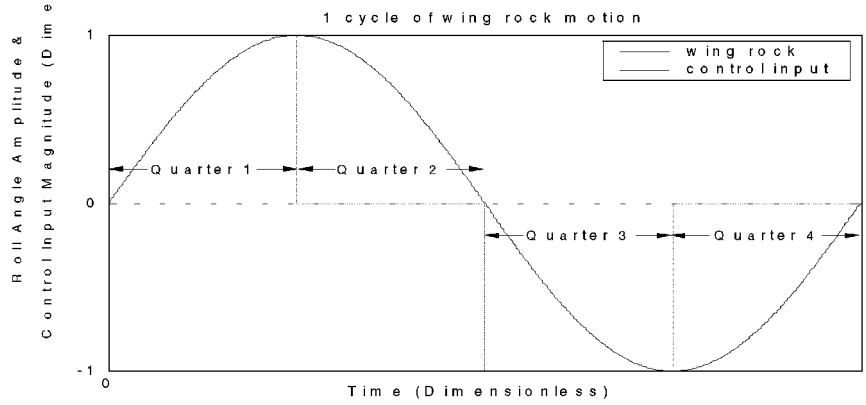

Fig. 3 Square-wave control input (RNLN).

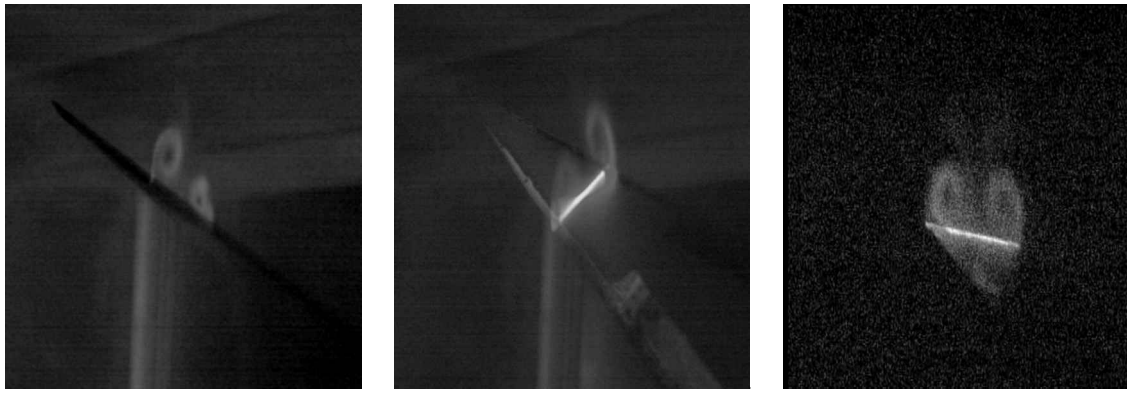

a) Maximum positive roll **b) Maximum negative roll** **c) Equilibrium**

Fig. 4 Flowfield at three static conditions.

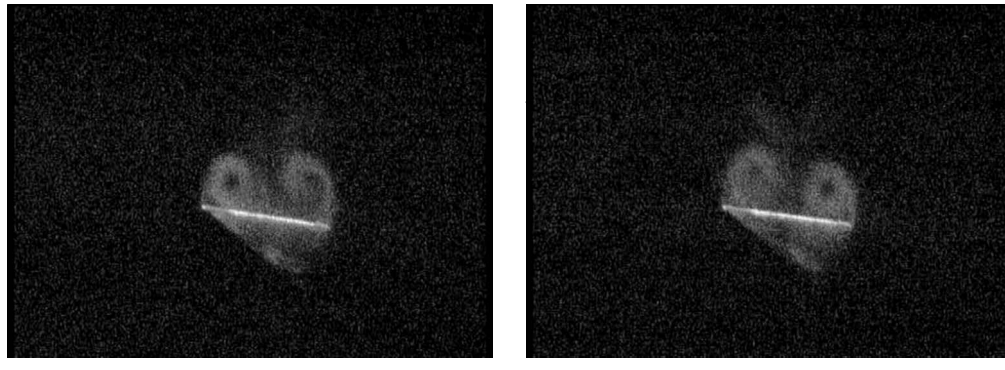

Fig. 5 Flowfield of static wing model subjected to blowing.

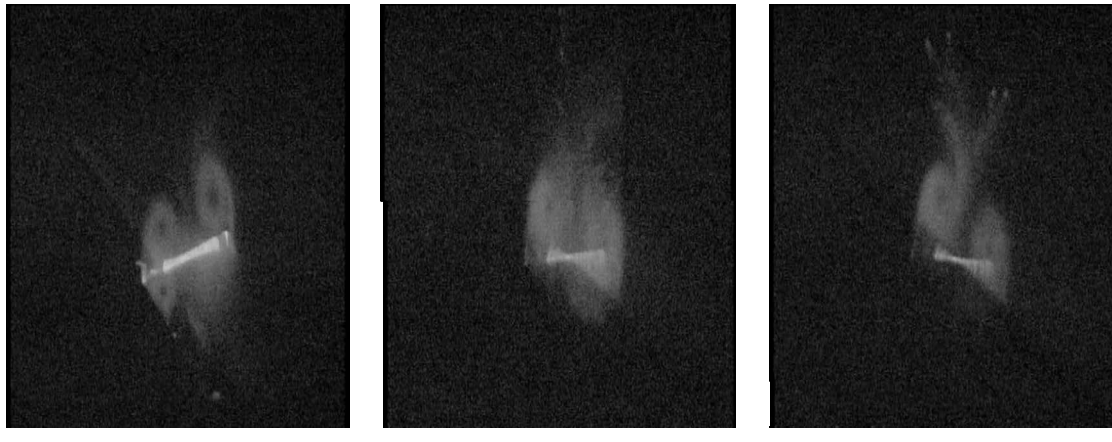

Fig. 6 Flowfield under dynamic wing rock motion.

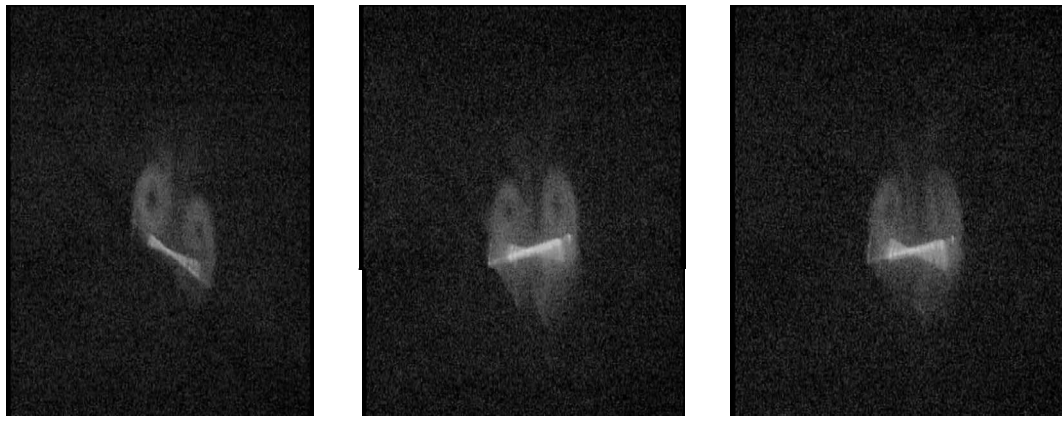

Fig. 7 Flowfield of model under dynamic wing rock motion and blowing RNLN.

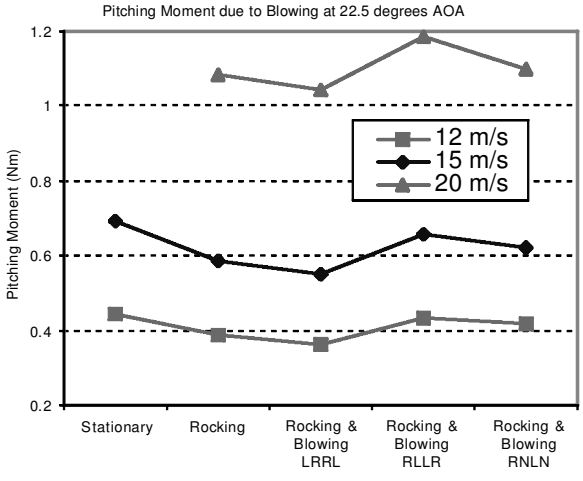

Fig. 8 Pitching-moment variation caused by blowing (at different U_0).

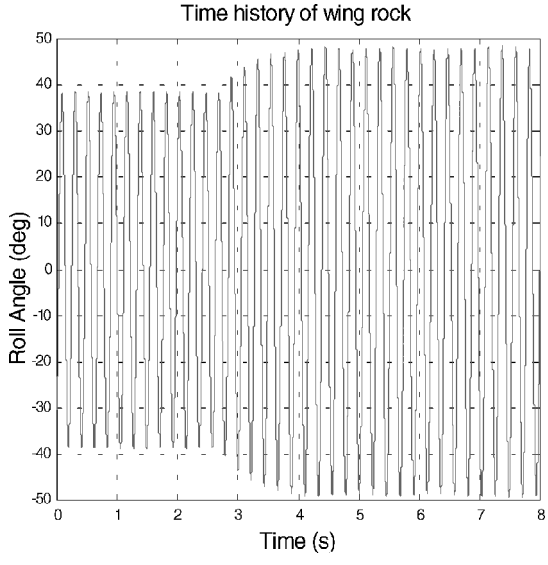

Fig. 9 Roll response with control input LRRL.

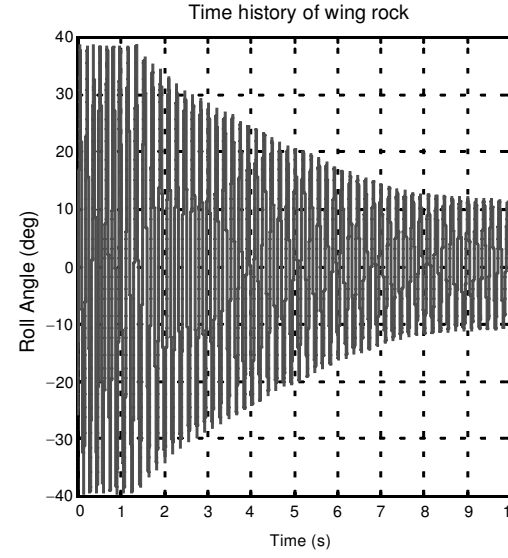

a) Decay of wing rock over 10 s

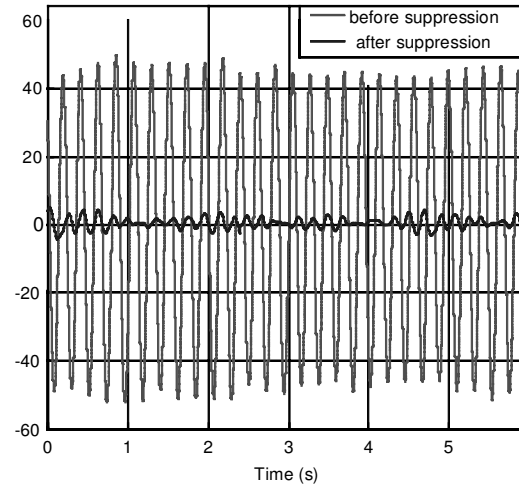

b) Amplitude of wing rock before and after suppression

Fig. 10 Roll response with control input RNLN.

where it is subjected to blowing. Furthermore, this vortex is lifted off from the wing surface so that it is slightly higher than the other vortex. Image b) shows the flowfield when the left wing is subjected to blowing. The result is analogous with the blowing on the right wing as seen by the vortex lifted off from the wing surface. The growth in the vortex size signifies that additional lift is generated as a result of blowing. Further examination of the flowfield under dynamic wing rock motion is undertaken to substantiate the findings.

Figure 6 illustrates the flowfield at three consecutive instants of time in one cycle of wing rock motion. These images substantiate the results that the vortex on the upper wing is bigger and further away from the wing surface, but is still attached to the wing. In addition, image b) shows that the vortices are almost symmetrical in size and position when the wing is passing through the zero roll position, which is at its maximum roll rate. Furthermore, it appears as though vortex breakdown is about to occur at this position.

Figure 7 illustrates the flowfield at three instants of time in one cycle of wing rock motion when it is subjected to the control input

of blowing RNLN. These images show that the vortices are reasonably symmetrical and well defined. Even when the wing is near the maximum roll amplitude, the vortices are almost symmetrical and level, as shown in image b). This set of control rule base was found to decrease the amplitude of wing rock.

The force balance experiment is conducted to establish the change in total pitching moment. The results are summarized in Fig. 8. The results indicated that the onset of wing rock causes a substantial decrease in the total pitching moment. Three sets of rule base are tested. They indicated that blowing LRRL further decreases the total pitching moment, whereas blowing RLLR and RNLN increases the total pitching moment. Generally, pitching moment is reduced when the amplitude of the rocking motion is amplified, and pitching moment is increased as the wing rock motion is weakened. Blowing LRRL increases the instability of the wing rock, whereas blowing RLLR or RNLN decreases its instability.

Figure 9 illustrates the roll response of blowing LRRL. The steady amplitude of wing rock reaches a higher value. The control input of blowing LRRL has aggravated the wing rock conditions and has resulted in an overall amplitude increase of about 25%.

Figure 10 illustrates the roll response of blowing RNLN. Figure 10a shows that the amplitude of wing rock is decaying over the time span of 10 s. Figure 10b shows the amplitude of the wing rock before suppression and after it is fully suppressed. The solid line indicates the amplitude of the wing rock after it is fully suppressed. This clearly demonstrates that the chosen rule base of RNLN with recessed angle blowing is very effective in suppressing the wing rock.

Conclusions

The roll response obtained shows that the wing rock amplitude increases as the control input of blowing LRRL is applied. Because this set of control input generates reaction force on the wing that opposes the wing rock motion, the increase in the wing rock amplitude must be caused by the adverse change in the vortices from the effects of blowing LRRL.

Conversely, the wing rock amplitude decays as the control input of blowing RNLN is applied. This set of control input generates reaction force on the wing that assists the wing rock motion. The decrease in the wing rock amplitude must be caused by the desired change in the vortices from the effects of blowing RNLN. The blowing coefficient is approximately estimated to be 0.033. The strength and positions of the vortices are affected by the blowing technique. The application of the RASB technique is to achieve a neutralization of the vortex asymmetry that occurs during wing rock. Arena and Nelson[7] stated that the hysteresis behavior in the normal position of the vortices is the prime candidate for the mechanism responsible for wing rock. During the wing rock motion, one vortex stays attached close to the wing surface while the other vortex goes through the vortex liftoff process to supply the wing rock mechanism. Flow visualization using the digital camera indicated that blowing causes the vortices to lift off from the wing surface. This observed change in the normal position of the vortex as a result of blowing is therefore an important criterion that might be responsible for the suppression of wing rock.

The effectiveness of the RASB technique lies in its ability to enlarge the associated vortex subjected to blowing and also to lift the vortex off the surface of the wing without causing vortex breakdown. Total lift over the wing is reduced on the onset of wing rock. The enlargement of the vortex subjected to blowing created the additional lift to restore the total lift to its original level. Vortex liftoff created the asymmetry necessary to initiate wing rock. The liftoff process of the vortex subjected to blowing counteracts this asymmetry to restore stability.

Acknowledgments

Authors would like to express thanks to Rik Heslehurst, Senior Lecturer, Australian Defence Force Academy, University of New South Wales for his suggestions in improving the presentation of the paper. We would like to place on record our appreciation for the reviewers for their suggestions for improving the presentation of the paper.

References

[1] Nayfeh, A. H., Elzebda, J. M., and Mook, D. T., "Development of an Analytical Model of Wing Rock for Slender Delta Wings," *Journal of Aircraft*, Vol. 26, No. 8, 1989, pp. 737–743.

[2] Ng, T. T., Suarez, C. J., and Malcom, G. N., "Forebody Vortex Control for Wing Rock Suppression," *Journal of Aircraft*, Vol. 31, No. 2, 1994, pp. 298–305.

[3] Johari, H., Olinger, D. J., and Fitzpatrick, K. C., "Delta Wing Vortex Control via Recessed Angled Spanwise Blowing," *Journal of Aircraft*, Vol. 32, No. 4, 1995, pp. 804–810.

[4] Johari, H., and Moreira, J., "Delta Wing Vortex Manipulation Using Pulsed and Steady Blowing During Ramp-Pitching," *Journal of Aircraft*, Vol. 33, No. 2, 1994, pp. 304–310.

[5] Arena, A. S., Nelson, R. C., and Schiff, L. B., "The Effect of Asymmetric Vortex Wake Characteristics on a Slender Delta Wing Undergoing Wing Rock Motion," AIAA Paper 89-3348, Aug. 1989.

[6] Arena, A. S., Nelson, R. C., and Schiff, L. B., "An Experimental Study of the Non-Linear Dynamic Phenomenon Known as Wing Rock," AIAA Paper 90-2812, Aug. 1990.

[7] Arena, A. S., and Nelson, R. C., "Experimental Investigation on Limit Cycle Wing Rock of Slender Wings," *Journal of Aircraft*, Vol. 31, No. 5, 1994, pp. 1148–1155.

Computational Investigation of Flow Through a Louvered Inlet Configuration

Ismail H. Tuncer*
Middle East Technical University, 06531 Ankara, Turkey
and
Max F. Platzer†
Naval Postgraduate School, Monterey, California 93943

Introduction

THE aerodynamic analysis of subsonic lifting body concepts for future unmanned air vehicles and missiles has been an active research field in recent years. A lifting body, as shown in Fig. 1, combines three emerging technologies, namely, lifting body, thrust vector control, and flush louvered inlet. The flush louvered inlet configuration requires the flow to turn 360 deg in the plenum chamber before entering the engine. The pressure losses and flow distortions experienced in the plenum chamber are serious concerns. In the analysis of the flow, the boundary-layer buildup on the underside of the missile body before reaching the louvered inlet and the three-dimensional flow in the plenum chamber are to be accounted for. Engine tests simulating flows through such an inlet configuration are currently not possible. It is, therefore, highly desirable to compute viscous, compressible flows through a typical flush louvered inlet configuration.

In this work, a numerical study of viscous, subsonic flow through a louvered inlet configuration is performed. In the design of louvered inlets, inlet vanes are required to achieve good total pressure recovery. However, in this analysis, the inlet vanes are not modeled

Presented as Paper 01-2477 at the AIAA 19th Applied Aerodynamics Conference, Anaheim, CA, 11–14 June 2001; received 31 January 2002; revision received 6 May 2002; accepted for publication 14 May 2002.

*Associate Professor, Department of Aerospace Engineering; tuncer@ae.metu.edu.tr. Member AIAA.

†Distinguished Professor, Department of Aero/Astronautics; platzer@aa.nps.navy.mil. Fellow AIAA.